



FATIGUE ANALYSIS USING THE FINITE ELEMENT METHOD

José Pereira R. Junior¹, Rene Q. Rodriguez², Simone dos S. Hoefel¹

¹*Dept. of Mechanical Engineering, Federal University of Piauí
Teresina, 64049-550, Piauí, Brazil*

josep9957@gmail.com, simone.santos@ufpi.edu.br

²*Dept. of Mechanical Engineering, Federal University of Santa Maria
Santa Maria, 97105-900, Rio Grande do Sul, Brazil
rene.rodriguez@ufsm.br*

Abstract. Fatigue failure analysis becomes a constant concern when intending to produce mechanical components subjected to alternating loads and stress concentration. Therefore, the study that provide the development of safe structures and with longer fatigue life proves to be of significant importance. This article presents the formulation of the finite element method applied to the fatigue problem in continuous structures from the modified Goodman, Gerber, and ASME-elliptic criteria. The stress field is obtained using a linear quadrilateral element, with four nodes per element and two degrees of freedom per node. It is considered two structures of optimized and non-optimized shape under boundary conditions of crimping and point loading at the free end. The numerical results obtained showed the effect of fatigue on the structures and among the various fatigue failure criteria. The modified Goodman criterion was more conservative, since it presented significantly higher results for the safety conditions considered, followed by the Gerber and, ASME-elliptic criteria, respectively.

Keywords: FEM, Fatigue failure, Stress, Continuous structures, Quadrilateral linear element.

1 Introduction

The study of fatigue began in the West in the 19th century after several disastrous train accidents, but it was in the 1990s that the subject gained greater prominence. This was mainly due to the growing use of critical components in industries such as automotive, high-speed rail, and aerospace (Smith and Hillmansen [1]).

In recent decades, several numerical modeling techniques have been used to analyze the behavior of complex structures, such as the Finite Element Method (FEM). Thus, it is possible to estimate the S-N curves of structures or their critical details, based on basic information on the fatigue strength of materials, resulting in a reduction in the time and cost of experimental tests. Deng et al. [2] applied the MEF to the study of fatigue failures in train tracks. In its formulation, the high cycle fatigue damage constitutive relationship of the Cement-emulsified Asphalt (CA) mortar was developed as a material subroutine, to incorporate into the finite element model for the influence of several key factors: such as void, initial deterioration, and a load of the wheel in the build-up of fatigue damage from the AC mortar. Pathak et al. [3] studied the fatigue of homogeneous plates and bimetals with interfacial cracks subjected to mechanical and thermal loads based on the Galerkin Method. Kumar et al. [4] modeled the crack growth in a single element for both isotropic and bimetals with the existence of inclusions and holes. Bhardwaj et al. [5, 6] analyzed the interfacial crack problem in heterogeneous materials and in materials with functional grading of two layers based on extended isogeometric analysis (XIGA).

More recently, researchers started to adopt topological optimization techniques to improve the performance of structures subjected to fatigue. Nabaki et al. [7] applied the Bidirectional Evolutionary Structural Optimization (BESO) method to minimize the volume of the structure subject to a fatigue constraint. Static failure and dynamic failure problems include stress singularity and many constraints, in addition to the highly non-linear behavior of stress with respect to design variables. Therefore, due to the non-linear nature of the constraint, the application of fatigue constraint in topology optimization is considered of high complexity among engineering problems. In this article, the MEF will be used to analyze fatigue failure factors in continuous structures based on different criteria,

including Modified Goodman, Gerber, and ASME-elliptic. Future work will be the topological optimization based on the aforementioned fatigue failure criteria.

2 Theoretical foundation

2.1 Finite Elements - Quad4 Linear Element

The structure is modeled with elastic linear quadrilateral isoparametric finite elements, with four nodes and two degrees of freedom per node (displacements in the vertical and horizontal directions). The elementary stiffness matrix is given by (Petyt [8]):

$$\mathbf{K} = \int_{-1}^{+1} \int_{-1}^{+1} h \mathbf{B}^T \mathbf{D} \mathbf{B} \det[\mathbf{J}] d\xi d\eta, \quad (1)$$

where, h is the thickness for out plane, \mathbf{B} , \mathbf{D} and \mathbf{J} are the strain, elasticity and Jacobian matrices, respectively. The equation of motion for a structure modeled using the MEF subject to static loads is given by:

$$\mathbf{K} \mathbf{U} = \mathbf{F}, \quad (2)$$

where, \mathbf{K} is the global stiffness matrix of the structure, \mathbf{U} is the displacement vector and \mathbf{F} is the force vector.

2.2 Fatigue Theory

When evaluating fatigue failure, the High Cycle Fatigue (HCF) approach is applied, the proportional sinusoidal load condition with constant amplitude is adopted, as shown in Fig. 1a. The stress state history shown in Fig. 1b is obtained by applying the sinusoidal load to the structure and then calculating the stress amplitude (σ_a) and the average stress (σ_m) from the maximum stress values (σ_{max}) and minimum (σ_{min}).

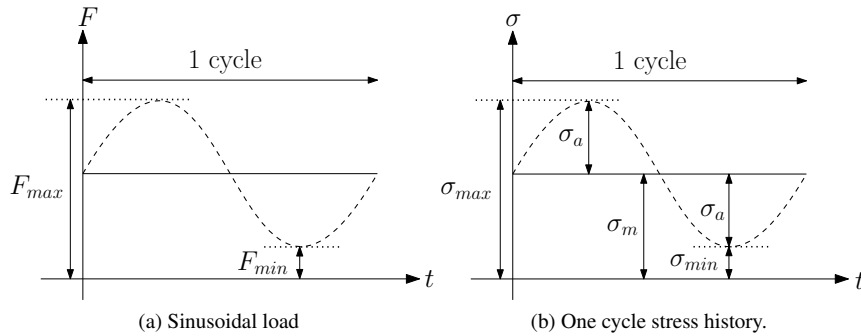


Figure 1. One cycle of the stress history in HCF.

Source: Adapted from Nabaki et al. [9].

However, equivalent static analysis is performed to assess fatigue failure. In this sense, the stresses vectors, σ_i , are calculated at the center of the element, as,

$$\sigma_i = \mathbf{D}_i \mathbf{B}_i \mathbf{u}_i, \quad (3)$$

where, u_i is the vector of nodal displacements of the element i . The alternating and mean stresses are calculated from the stress values being expressed by:

$$\sigma_{a_i} = c_a \sigma_i = \begin{bmatrix} \sigma_{x_{a_i}} \\ \sigma_{y_{a_i}} \\ \tau_{xy_{a_i}} \end{bmatrix} \quad \text{and} \quad \sigma_{m_i} = c_m \sigma_i = \begin{bmatrix} \sigma_{x_{m_i}} \\ \sigma_{y_{m_i}} \\ \tau_{xy_{m_i}} \end{bmatrix}, \quad (4)$$

where, c_a and c_m are, respectively, amplitude and mean scaling factors given by:

$$c_a = \frac{1 - (F_{min}/F_{max})}{2} \quad \text{and} \quad c_m = \frac{1 + (F_{min}/F_{max})}{2}. \quad (5)$$

The von-Mises stress calculation is used to calculate the mean and alternating stress of the elements as follows:

$$\begin{aligned}\sigma_{a_i}^{\text{vonMises}} &= \sqrt{\sigma_{x_{a_i}}^2 + \sigma_{y_{a_i}}^2 - \sigma_{x_{a_i}} \sigma_{y_{a_i}} + 3\tau_{xy_{a_i}}^2}, \\ \sigma_{m_i}^{\text{vonMises}} &= \sqrt{\sigma_{x_{m_i}}^2 + \sigma_{y_{m_i}}^2 - \sigma_{x_{m_i}} \sigma_{y_{m_i}} + 3\tau_{xy_{m_i}}^2}.\end{aligned}\quad (6)$$

The assessment of fatigue failure is made by applying the modified Goodman, Gerber and ASME-elliptic criteria, given by:

$$L_i^{GM}(x) = \frac{\sigma_{a_i}^{\text{vonMises}}}{(\sigma_i)_{N_f}} + \frac{\sigma_{m_i}^{\text{vonMises}}}{\sigma_{ut}} \leq 1 \quad (7)$$

$$L_i^G(x) = \frac{\sigma_{a_i}^{\text{vonMises}}}{(\sigma_i)_{N_f}} + \left(\frac{\sigma_{m_i}^{\text{vonMises}}}{\sigma_{ut}}\right)^2 \leq 1 \quad (8)$$

$$L_i^{AE}(x) = \left(\frac{\sigma_{a_i}^{\text{vonMises}}}{(\sigma_i)_{N_f}}\right)^2 + \left(\frac{\sigma_{m_i}^{\text{vonMises}}}{\sigma_{ut}}\right)^2 \leq 1. \quad (9)$$

For the fatigue failure criteria based on principal stresses, the diagram in Fig. 2 is used, where the alternating stress is limited by the critical fatigue stress, $(\sigma_i)_{N_f}$, considering an infinite number of lifecycles ($N_f > 10^7$). To avoid fatigue failure, all combinations of alternating stress and average stress of all elements in the structure must be below the diagram curves (Fig. 2), where, σ_{ut} and σ_y represent ultimate stress and yielding stress, respectively.

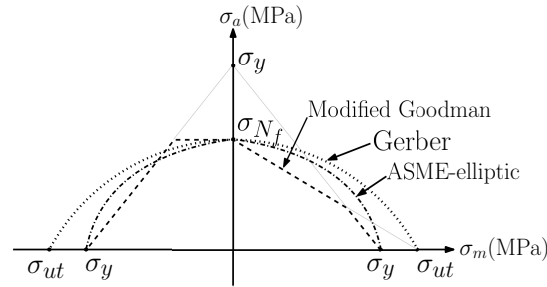


Figure 2. Diagram of fatigue failure criteria.

The value of the alternating stress $(\sigma_i)_{N_f}$, is obtained through the Basquin equation (Nabaki et al. [9]) written as:

$$(\sigma_i)_{N_f} = \sigma'_f (2N_f)^b, \quad (10)$$

where, σ'_f and b are, the fatigue strength coefficient and exponent, respectively.

To verify the failure resistance of the structures, three different combinations of average and alternating principal stresses are considered, where the results from these combinations, in each element, are placed in the diagram. Combinations of medium and alternating stress are written as follows (Nabaki et al. [9]):

Combination 1:

$$\sigma_a = \sqrt{\sigma_{1a}^2 + \sigma_{2a}^2 - \sigma_{1a}\sigma_{2a}} \quad \text{and} \quad \sigma_m = \sqrt{\sigma_{1m}^2 + \sigma_{2m}^2 - \sigma_{1m}\sigma_{2m}}, \quad (11)$$

Combination 2:

$$\sigma_a = \sqrt{\sigma_{1a}^2 + \sigma_{2a}^2 - \sigma_{1a}\sigma_{2a}} \quad \text{and} \quad \sigma_m^{eq} = \sigma_{1m} + \sigma_{2m}, \quad (12)$$

Combination 3:

$$\begin{aligned}\sigma_a &= \sqrt{\sigma_{1a}^2 + \sigma_{2a}^2 - \sigma_{1a}\sigma_{2a}} \quad \text{and} \\ \sigma_m^{\text{signed vonMises}} &= \begin{cases} \sqrt{\sigma_{1m}^2 + \sigma_{2m}^2 - \sigma_{1m}\sigma_{2m}} & \text{if } |\sigma_{1m}| \geq 0 \\ -\sqrt{\sigma_{1m}^2 + \sigma_{2m}^2 - \sigma_{1m}\sigma_{2m}} & \text{if } |\sigma_{1m}| < 0 \end{cases}.\end{aligned}\quad (13)$$

3 Methodology

In this paper we implemented the stress calculation routine and the modified Goodman, Gerber and ASME-elliptic criteria via a finite element analysis package, in MATLAB environment, provided by Picelli et al. [10] and available on the online repository (here). The SolidWorks software is used to delineate and dimension structures of optimized geometry found in the literature, arriving at an approximate geometry. Then, the sketch is imported to the Abaqus software, where the structure is discretized with the Quad4 element. Finally, the coordinates of each node are gathered, added to the pre-processing of the aforementioned computational programming, in which you get the answers to each problem.

4 Results

In order to validate the computational code and obtain new results, two structures are considered, the cantilever beam (Fig. 3a) and the L beam (Fig. 3b). In both, 1 mm is defined as the thickness for out plane, modulus of elasticity and Poisson’s coefficient, as 210 GPa and 0.3, respectively. The statically applied load was considered as $F = F_{max}$. To construct the failure criteria diagrams, the parameters $\sigma'_f = 493$ MPa, $\sigma_{ut} = \sigma_y = 358$ MPa, $N_f = 1e7$ and $b = -0.086$ are used. In addition, discretization with Quad4 elements (1 mm x 1 mm) is used. In the validation stage, the results obtained by the authors of this work were compared to those found in the literature for the same structure.

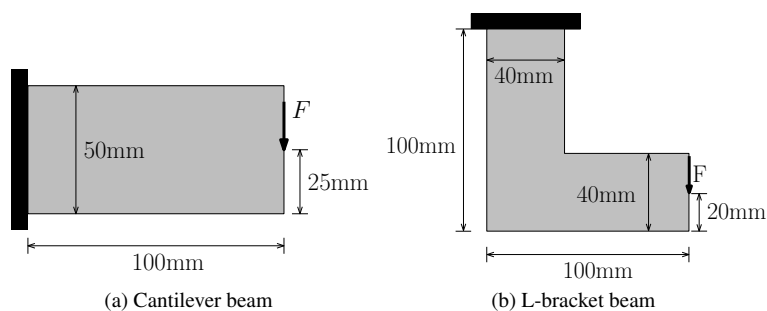
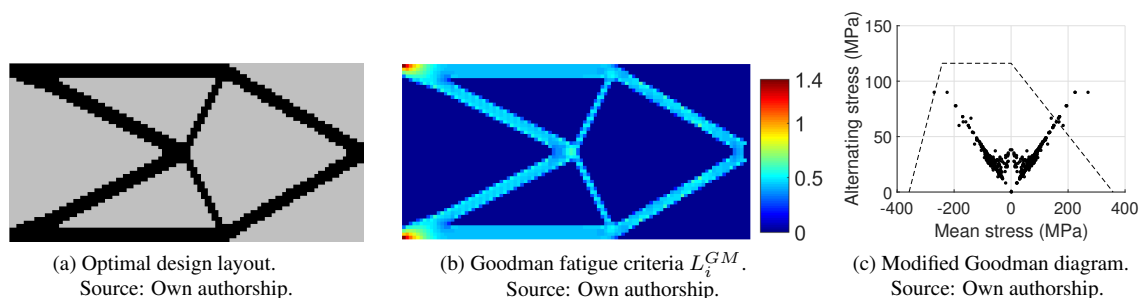


Figure 3. Beam models.

4.1 Validation 01 - Optimized Cantilever Beam

In this section, the cantilever beam is considered, with dimensions, boundary conditions and point load shown in Fig. 3a, where $F_{max} = 350$ N and $F_{min} = 150$ N. Nabaki et al. [9] optimize this structure via BESO, with volume restriction. With this, they obtained the layout of Fig. 4a, as well as the results in Fig. 4b and 4c. Using a similar layout (Fig. 4d), the authors of the present work obtained the results in Fig. 4e and 4f, through the MEF in the computational code in MATLAB. The colors in the geometry domain (Fig. 4b and 4e) represent the distribution of the values L_i in the structure and the colors highlight the critical regions of the structure, values of L_i greater than or equal to one indicate fatigue failure. Figures 4c and 4d present the modified Goodman diagram, in which the fatigue analysis is considered from the mean and alternating principal stresses. In these figures (4c and 4d), points outside the the safety zone of the diagram, that is, outside the region delimited by the dashed lines, indicate fatigue failure.



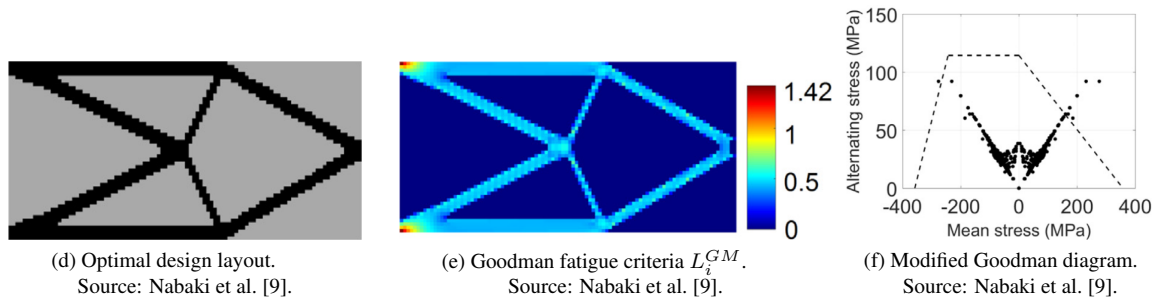


Figure 4. Validation of results for the cantilever beam.

The results in Fig. 4b and 4e, indicate failure in the structure due to fatigue, as they present values of L_i^{GM} greater than one, the same conclusion can be made when evaluating the Fig. 4c and 4f, they contain points outside the safety zone of the modified Goodman diagram. When comparing the results of the present work and the literature, similarities can be seen in the color maps (Fig. 4b and 4e), as well as in the arrangement of points in the modified Goodman diagrams (Fig. 4c and 4f). Therefore, there is good agreement in the results. Furthermore, small differences are present and are due to the there is no exact match between layouts (Fig. 4a and Fig. 4d).

4.2 Validation 02 - Optimized L-Beam

The second example is the L-beam, with dimensions, boundary conditions and loading conditions shown in Fig. 3b, where $F_{max} = 250\text{ N}$ and $F_{min} = 50\text{ N}$. Using this structure in the BESO method, with volume restriction, Nabaki et al. [9] found the layout of Fig. 5a and the results in Fig. 5b and 5c. With a similar structure (Fig. 5d) the authors of the present work obtained the answers in Fig. 5e and 5f based on the same procedures mentioned in the first example.

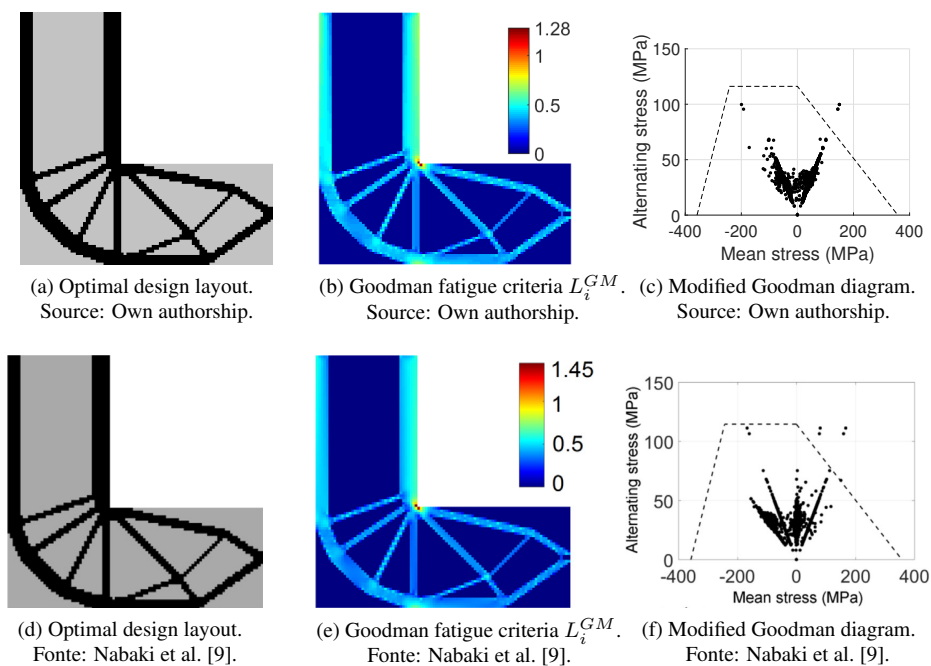


Figure 5. Validation of results for the L-Bracket.

From the results in Fig. 4b and 4e, as well as in Fig.4c and 4f, it can be seen that the structure fails due to fatigue. The aspect of Fig. 4b and 4e which reveals the distribution of the values L_i^{GM} in the structure are similar. However, due to the geometric arrangement of the structure, the mesh becomes dependent on small changes, promoting some dissimilarities in the results, subtle between Fig. 4b and 4e, notable among the Fig. 4c and 4f. However, the results were satisfactory in showing fatigue failure, thus confirming the assertiveness of the computational code.

4.3 Application 01 - Cantilever beam not optimized

To evaluate the fatigue failure responses of various criteria, the cantilever beam (Fig. 3a), a non-optimized structure, is used as a first example with load values $F_{max} = 350$ N and $F_{min} = 150$ N. Figure 6 presents the responses of Goodman, Gerber and ASME-elliptic fatigue failure criteria. In these graphs, the effects of stress concentration are disregarded, 10 elements in the vicinity of the force are disregarded from the calculation of the failure criteria.

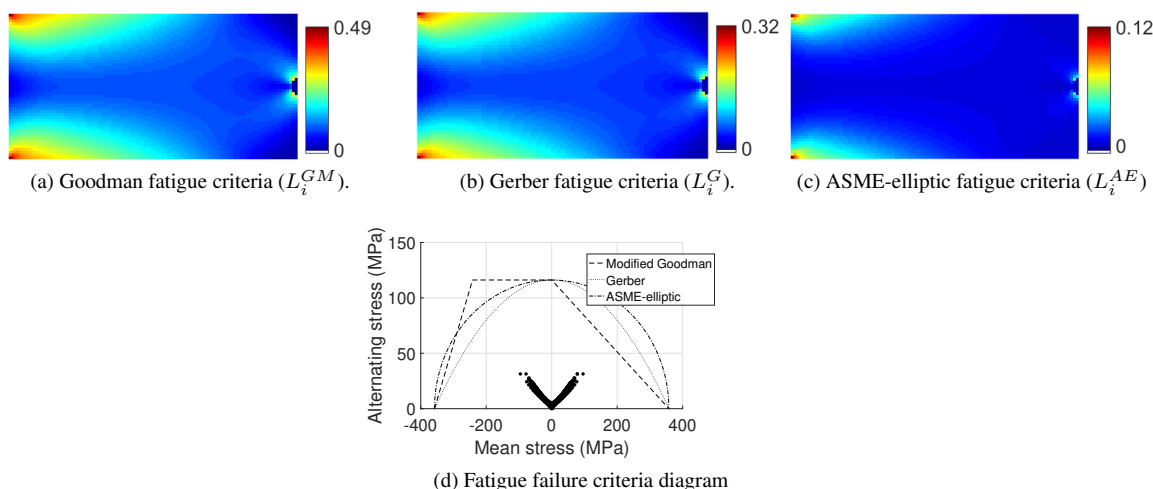
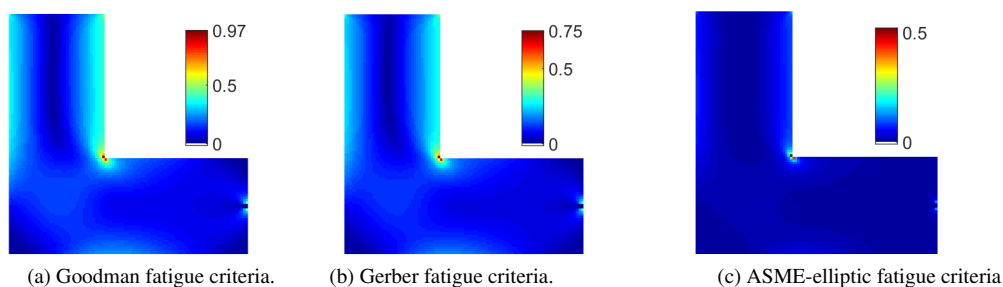


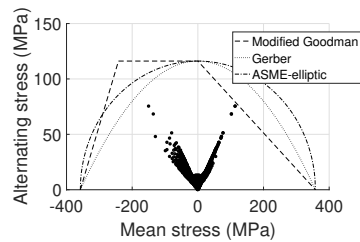
Figure 6. Results for the cantilever beam.

It can be seen in the example considered that there is no failure due to fatigue, there are $L_i < 1$ in all answers. At the left end, converging to the upper and lower vertices, are the regions of greatest expressiveness, that is, the highest values of L_i . Comparing the criteria, the modified Goodman (Fig. 6a) presented the highest values, followed by the Gerber criterion (Fig. 6b), and ASME-elliptic (Fig. 6a), respectively. Modified Goodman, therefore, is among the criteria the most conservative, highlighting more intensely the possibility of failure due to fatigue. The evaluation from the average and alternating principal stresses are shown in Fig. 6d. In this diagram, the fatigue resistance of the structure is again shown, since all points are in the safe zone of the diagram, that is, below the fatigue failure curves.

4.4 Application 02 - L-beam not optimized

As a second example, the L-bracket beam is used (Fig. 3b), with load values $F_{max} = 250$ N and $F_{min} = 50$ N. To avoid stress concentration, six elements (3×2) around the applied load were excluded from the calculation of the failure criteria. According to Fig. 7a, 7b and 7c, none of the criteria shows fatigue failure in the considered example. It is also noticed that the maximum values found, in the structure domain, are located near the upper vertex formed by the vertical and horizontal portions.





(d) Fatigue failure criteria diagram

Figure 7. Results for the L-Bracket.

In the modified Goodman results (Fig. 7a), there are maximum values close to 0.97, thus the structure is safe, however close to the limit conditions of failure resistance. Gerber results present maximum values close to 0.75 and ASME-elliptic close to 0.5, showing that there is no failure. It can be seen, therefore, that Goodman moddicated presents greater numerical expressiveness, values of L_i^{GM} greater than L_i^G and L_i^{AE} . In its turn, the failure criteria diagram, Fig. 7d, reaffirms the resistance of the structure to failure due to fatigue, since the points are in the safe zone of the diagram.

5 Conclusions

Fatigue damage in continuous structures was evaluated based on the modified Goodman, Geber and ASME-elliptic failure criteria via FEM. Optimized geometry structures known in the literature were used in the implemented computational code. Results obtained were in well agreement with those presented on previous work. Further, two non-optimized structures (cantilever and L-beam) were evaluated. For the conditions placed, they did not show fatigue failure in the evaluation criteria. It was also verified that the modified Goodman criterion presents more expressive values, followed by the Gerber and ASME-elliptic criterion, that is, $L_i^{GM} > L_i^G > L_i^{AE}$. Therefore, modified Goodman criterion emphasizes more intensely the presence of failure due to fatigue.

Acknowledgements. J. P. R. J. acknowledges ABCM for scholarship support.

Authorship statement. The authors hereby confirm that they are the sole liable persons responsible for the authorship of this work, and that all material that has been herein included as part of the present paper is either the property (and authorship) of the authors, or has the permission of the owners to be included here.

References

- [1] R. Smith and S. Hillmansen. A brief historical overview of the fatigue of railway axles. *Proceedings of the Institution of Mechanical Engineers, Part F: Journal of Rail and Rapid Transit*, vol. 218, n. 4, pp. 267–277, 2004.
- [2] S. Deng, J. Ren, K. Wei, W. Ye, W. Du, and K. Zhang. Fatigue damage evolution analysis of the ca mortar of ballastless tracks via damage mechanics-finite element full-couple method. *Construction and Building Materials*, vol. 295, pp. 123679, 2021.
- [3] H. Pathak, A. Singh, and I. V. Singh. Fatigue crack growth simulations of homogeneous and bi-material interfacial cracks using element free galerkin method. *Applied Mathematical Modelling*, vol. 38, n. 13, pp. 3093–3123, 2014.
- [4] S. Kumar, I. Singh, B. Mishra, and T. Rabczuk. Modeling and simulation of kinked cracks by virtual node xfem. *Computer Methods in Applied Mechanics and Engineering*, vol. 283, pp. 1425–1466, 2015.
- [5] G. Bhardwaj, I. Singh, and B. Mishra. Stochastic fatigue crack growth simulation of interfacial crack in bi-layered fgms using xiga. *Computer Methods in Applied Mechanics and Engineering*, vol. 284, pp. 186–229, 2015.
- [6] G. Bhardwaj, S. Singh, I. Singh, B. Mishra, and T. Rabczuk. Fatigue crack growth analysis of an interfacial crack in heterogeneous materials using homogenized xiga. *Theoretical and Applied Fracture Mechanics*, vol. 85, pp. 294–319, 2016.
- [7] K. Nabaki, J. Shen, and X. Huang. Bi-directional evolutionary topology optimization based on critical fatigue constraint. *International Journal of Civil and Environmental Engineering*, vol. 12, n. 2, pp. 113–118, 2018.
- [8] M. Petyt. *Introduction to finite element vibration analysis*. Cambridge university press, 2010.
- [9] K. Nabaki, J. Shen, and X. Huang. Evolutionary topology optimization of continuum structures considering fatigue failure. *Materials & Design*, vol. 166, pp. 107586, 2019.
- [10] R. Picelli, S. Ranjbarzadeh, R. Sivapuram, R. Gioria, and E. Silva. Topology optimization of binary structures under design-dependent fluid-structure interaction loads. *Structural and Multidisciplinary Optimization*, vol. 62, n. 4, pp. 2101–2116, 2020.